Biosensors and Bioelectronics 199 (2022) 113887

Contents lists available at ScienceDirect

Biosensors and Bioelectronics

journal homepage: www.elsevier.com/locate/bios

Extending lifetime of gas-phase odor biosensor using liquid thickness control and liquid exchange

Hongchao Deng [a], Hidefumi Mitsuno [b], Ryohei Kanzaki [b], Takamichi Nakamoto [a,*]

[a] Laboratory for Future Interdisciplinary Research of Science and Technology (FIRST), Institute of Innovative Research (IIR), Tokyo Institute of Technology, 4259 Nagatsuta-cho, Midori, Yokohama, Kanagawa, 226-8503, Japan
[b] Research Center for Advanced Science and Technology (RCAST), The University of Tokyo, 4-6-1 Komaba, Meguro, Tokyo, 153-8904, Japan

ARTICLE INFO

Keywords:
Gas phase
Odorant detection
Olfactory receptor
Feedback control
Liquid exchange
Biosensor

ABSTRACT

In recent few years, researchers utilized cell expressing olfactory receptor for vapor detection under various sensing mechanisms. Those olfactory systems, however, have relatively short lifetime due to the dry out of aqueous solution covering the cell. In this paper, we came up with a feedback control structure composed of an impedance measurement circuit, a microcontroller and two syringe pumps for maintaining thin liquid layer above cell. Cell lifetime was improved from less than 40 min to longer than 75 min when liquid film control was introduced. However, the biosensor lifetime remained similar between with or without liquid thickness control. Then, we added liquid exchange to further extend the lifetime of our odor biosensor. Minimal liquid exchange speed was able to significantly extend the biosensor lifetime. Meanwhile, faster liquid exchange speed resulted in better sensor responses. Furthermore, the enhancement acquired from intermittent liquid exchange was compared with continuous one. In this study, the lifetime of odor biosensor was extended to more than 3 h whereas it was less than half an hour without liquid thickness control. We believe the methodology we established in this paper will facilitate gas phase odor biosensor in continuous monitoring of target substances.

1. Introduction

The atmosphere is full of various odor molecules. Those odorants not only influence the behavior of animals, but also transmit essential information about the environment (Nielsen et al., 2015; Su et al., 2020; Sukekawa et al., 2019). Thus, odor sensing systems using various types of sensors such as quartz crystal microbalance (QCM) sensor, metal oxide sensor, conducting polymer sensor, surface acoustic wave (SAW) sensor, and electrochemical sensor have been studied for long time (Ema et al., 1989; Nakamoto, 2016; Pearce et al., 2002; Persaud and Dodd, 1982). However, it is not easy to develop sensors with sufficient sensitivity and selectivity. Attracted by the high sensitivity and selectivity of creatures' olfaction, scientists attempted to fabricate sensors with various biological materials (Khadka et al., 2019; Lim et al., 2013; Wu et al., 2009). Among them, the living olfactory sensory neurons (OSNs) obtained from animals or transfected cells expressing olfactory receptors (ORs) drew the attention of many researchers (Datta-Chaudhuri et al., 2016; Mitsuno et al., 2015; Sato and Takeuchi, 2014; Sukekawa et al., 2021). Compared with sensory neuron, the transfected cell method allows the creation of a stable cell line capable of keeping similar sensitivity and selectivity for long time, also any type of OR can be chosen for expression on the cell membrane. Therefore, this technique is more admired for designing odor biosensors lately.

The cell expressing OR requires the aqueous environment to ensure the function of OR protein. Hence, previous odor biosensors using reconstituted ORs were mainly used to detect odorant molecules dissolved in liquid phase (Fig. 1a). However, the applications to the sensors only in the liquid phase were very limited. Recently, researchers expanded their application scenarios to gas phase (Kida et al., 2018; Lee et al., 2015; Sato and Takeuchi, 2014). The liquid layer mimicking mucus layer above OR is required even for the biosensor used in the gas phase. Since majority of odorant molecules are hydrophobic, they cannot easily penetrate thick liquid layer. A sufficiently thin liquid film is demanded for detecting gas phase odorant directly (Fig. 1b). Till now, there is no method for maintaining such thin liquid layer in those gas phase odor biosensors. Investigators need to make a balance between better response and longer lifetime accordingly.

An odor biosensor for gas phase odorant detection was established in our previous research (Deng et al., 2021). Thin liquid layer introduced sensitive and rapid OR response. However, experiments terminated

* Corresponding author.
E-mail address: nakamoto.t.ab@m.titech.ac.jp (T. Nakamoto).

https://doi.org/10.1016/j.bios.2021.113887
Received 13 October 2021; Received in revised form 9 December 2021; Accepted 10 December 2021
Available online 12 December 2021
0956-5663/© 2021 The Authors. Published by Elsevier B.V. This is an open access article under the CC BY license (http://creativecommons.org/licenses/by/4.0/).

within around 11 min because assay buffer solution dried out fast. Inspired by the animals' olfactory system whose OSNs are all covered by thin layer of mucus or lymph (Johnson, 2011; Leal, 2013), a stable liquid thickness is indispensable for improving the performance of our odor biosensor. To realize this, one way is to supply liquid in a fixed flow rate—also named as open loop control—into the cell area for compensating the evaporated water. This method is easy to implement but the liquid evaporation speed could be affected by multiple environmental factors such as temperature, humidity, and gas flow velocity. Thence, the suitable compensation rate is hard to determine. On the other hand, feedback control adjusts the liquid supplementary speed according to the real-time measurement result. It can preserve steady liquid thickness level with a proper controller for calculating control signal, an actuator for adding/removing liquid, and a sensor for sensing the liquid thickness alteration. In this study, a microcontroller and two syringe pumps were used as controller and actuator. As for liquid thickness measurement, plenty of techniques including total internal laser reflection (Hurlburt et al., 1995), superimposed ultrasonic standing wave (Kanja et al., 2021), wire-mesh (Da Silva et al., 2007), electrode matrix and so on are well developed (Thiele et al., 2009). Since only monitoring of liquid layer relative variation was required here, a pair of electrodes with impedance measurement circuit were fabricated as the sensor.

In this paper, we upgraded our olfactory system with liquid thickness control and liquid exchange (Fig. 1c). The liquid thickness control preserved cells submerge into buffer solution, thereby guaranteeing cell activity for long time. An intermittent or continuous liquid flow was implemented during the experiment to refresh buffer medium in cell area. In view of this, reproducible OR responses could be received under a series of target odorant stimulations. In addition, we checked our sensor system responses towards distinct agonist densities to further demonstrate the effectiveness of liquid thickness control and liquid exchange, which have never been reported as far as we know.

2. Material and methods

2.1. Experiment chamber

A method for sensing the liquid thickness variation by measuring the impedance between two electrodes was applied here. As shown in Fig. 2a, a piece of tape (thickness: 0.085 mm) with 8 mm × 8 mm hole as cell area cut by cutting plotter (CE600, Graphtec) was pasted to a glass slide (thickness: 1.3 mm). 10 μl assay buffer solution (140 mM NaCl, 5.6 mM KCl, 4.5 mM $CaCl_2$, 11.26 mM $MgCl_2$, 11.32 mM $MgSO_4$, 9.4 mM D-glucose, 5 mM HEPES, pH 7.2) with cell was left in the hole area which means the estimated liquid thickness was 156.25 μm. Two beryllium bronze electrodes with spring (Φ: 0.68 mm, Walfront) contacting with bottom of cell area were chosen for impedance measurement. Two stainless tubes (Φ: 0.55 mm, Nilaco) submerged into buffer solution were used for liquid input and output. The target odorant was supplied from a Teflon tube (Φ: 1 × 2 mm, Naflon) and the outlet of the odorant port was 3 mm above the cell area. The microscope glass slide, electrodes, stainless tubes and Teflon tube were all fixed in a holder (Fig. 2b). The impedance between two electrodes increased with the liquid evaporation. Hence, the impedance value acquired by the measurement circuit represented the liquid thickness level.

2.2. Feedback control structure

Fig. 2c illustrates the mechanism of feedback control method. In the outset of an experiment, the impedance value was recorded once as the set point. During the experiment, the difference between set point and current value was input into the microcontroller (Arduino Nano, Arduino). The microcontroller tweaked the control signal based on proportional–integral–derivative (PID) algorithm (mainly proportional control) to modulate the motor driver (L6470, Strawberry Linux) thus controlling syringe pump (LPDA2750125D, Lee Company) infusing or withdrawing liquid (see supplementary material for detail). The buffer solution discharged from the syringe pump compensated the evaporated water therefore reduced the impedance value towards set point. For mitigating the noise and disturbance, the abnormal control signal was discarded, and the impedance was measured twelve times and the maximum/minimum values were removed then calculated the average value as current value. It took around 0.24 s to compute a new control signal.

2.3. Sensing element and target odorant preparation

The sensing element and odorant preparation procedure used here were the same as our previous study. Briefly, the *Spodoptera frugiperda* cell (Sf21) co-expressing OR, OR co-receptor (Orco), and calcium-sensitive fluorescence protein (GCaMP6s) was applied as basic sensing element (Chen et al., 2013; Termtanasombat et al., 2016). The OR we chose was Or13a from fruit-fly, *Drosophila melanogaster*. Unlike OR from vertebrates, insect OR with Orco forms the ion channel thus can directly induce the ion influx. After Or13a is combined with its agonist, an ion channel opens then starts a Ca^{2+} inflow. The fluorescent intensity from GCaMP6s increases with calcium ion concentration. Therefore, the difference of fluorescent brightness between peak and initial value after target odorant stimulation was regarded as OR response. According to the property of Or13a (Münch and Galizia, 2016), 1-octen-3-ol was selected as target odorant. Benefits from the 50 nM detection limit of Or13a towards 1-octen-3-ol (Mujiono et al., 2017), detection of 1-octen-3-ol vapor is feasible in spite of its insoluble property in aqueous solution.

For the preparation of gas phase odorant samples, 1-octen-3-ol (O5284, Sigma-Aldrich) was diluted into intended concentrations by non-volatile liquid, i.e., decanoyl/octanoyl-glycerides and stored in pierce vial (3.5 mL, AS ONE) for later experiments. The headspace gas of sample vials was adopted for target odorant stimulation and the vapor concentrations (v/v) of various liquid samples were evaluated in our previous research (Deng et al., 2021).

2.4. Experiment system and procedure

The schematic diagram of experiment system is shown in Fig. 2d. Before the experiment started, the odorant sample bottle was connected

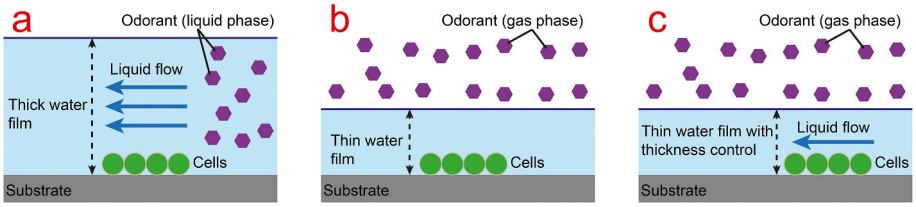

Fig. 1. Mechanisms of odorant detection. (a) Odorant is dissolved into liquid phase then applied to cell. (b) Odorant is directly detected in gas phase under thin liquid film. (c) Odorant is directly detected in gas phase under thin liquid film, liquid thickness control and liquid exchange (manifesting as liquid flow) methods are utilized for extending the biosensor lifetime.

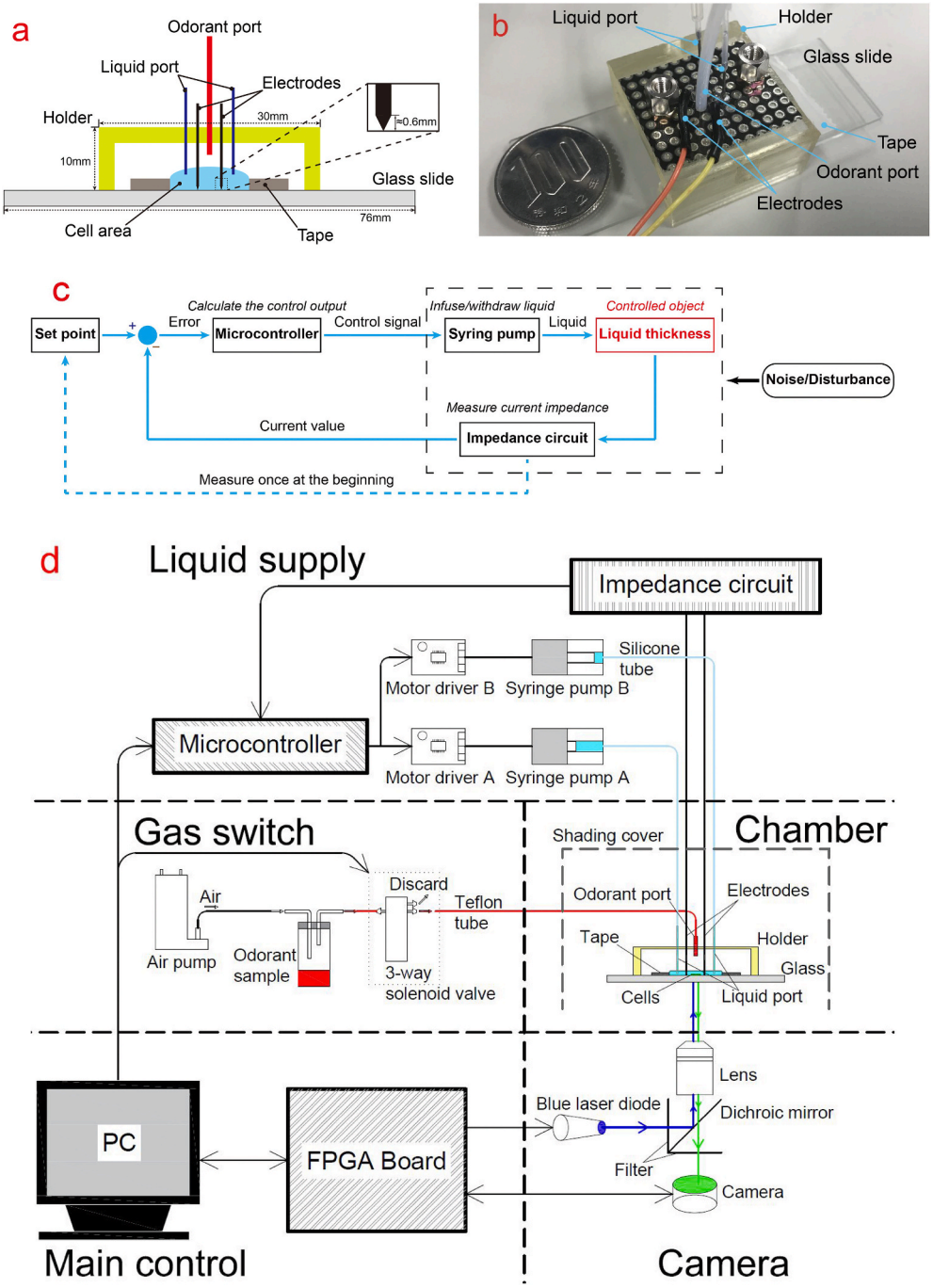

Fig. 2. Illustration of experiment system. (a) schematic of experiment chamber. (b) an image of experiment chamber. (c) Mechanism of feedback control method. The blue dash line from "Impedance circuit" to "Set point" represents the measurement only happens once at the beginning of experiment, whereas the blue solid line means they continue the entire experiment. The black dotted box indicates the components affected by noise and disturbance. (d) The structure of measurement system. (For interpretation of the references to colour in this figure legend, the reader is referred to the Web version of this article.)

to the air channel. The air pump flowed the air into headspace of sample bottle at 55 mL/min continuously. The PC determined whether the target odorant was provided to chamber or discarded. A 70 cm Teflon tube was connected between solenoid valve (EXAK-3, Takasago Denki) and odorant port. The flow channel was rinsed with sample gas for 30 s.

Sf21 cells were harvested and suspended with assay buffer solution then loaded into the cell area. For the sake of reducing the individual differences among cells, the cell number captured by camera was normally larger than 200. We waited for 6 min for cell adhesion then removed extra liquid containing floating cells. Finally, a shading lid was covered above chamber for mitigating the influence from ambient light.

The start signal was sent from PC to its peripherals. The microcontroller began to control the liquid thickness level once the test initiated. Syringe pump A infused liquid at the speed of the summation of liquid compensation and exchange. Syringe pump B extracted the buffer solution at the rate of liquid exchange. The combination of pump A and B compensated the evaporated water as well as established liquid exchange in cell area. The minimum pump speed was 1 step/tick—which equals 0.1588 μl/min—and only could change in integer multiples.

When the solenoid valve turned on, the headspace gas of odorant sample vessel was supplied to cells below odorant port, thus introduced an OR response. The interval between two stimulations was 500 s and during this period there was no gas flow inside the Teflon tube. The cell fluorescence image was recorded every 2 s by camera module (OV7740, OmniVision) and transferred to PC for subsequent analysis.

The OR response caused by target odorant was calculated based on the fluorescence brightness change. The magnitude of a response was calculated by the following formula:

$$Response = \frac{B_{peak} - B_{initial}}{B_{initial}} \quad (1)$$

where $B_{initial}$, B_{peak} are initial and peak brightness after stimulation, respectively. In order to reduce the noise from background area, we used the circle Hough transform in Matlab to extract cell region then computed the luminance variation.

3. Results and discussion

3.1. Measuring frequency and typical impedance curve

The core component in our homemade impedance measurement board is an impedance converter (AD5933, Analog Devices) which can measure the impedance from 10 to 100 kHz. Thus, we should determine the optimal working frequency for the following experiments.

The impedance value between 10 and 100 kHz with 1 kHz interval was recorded around every 30 s after loading buffer solution containing cells into cell area. Fig. S1 shows the measured impedance values of all frequencies. The impedance tendency was quite similar in whole frequency range while the relative change increased with frequency. Although the maximum relative change frequency altered among different tests, considering that larger measuring frequency could lead to shorter sampling time, 100 kHz was chosen for subsequent experiments accordingly.

Fig. S1 illustrates that the impedance raised slowly with time before 300 s, if more liquid was remained in cell area, such gentle impedance change would last longer. When the liquid layer becomes much thinner, tiny thickness variation leads to large impedance alteration. For the sake of favorable system stability, we remained 10 μl medium in cell area. In this condition, the impedance value could stay in mild change region over time for an enough long period.

3.2. Extend cell lifespan by maintaining liquid layer

To extend the lifetime of our odor biosensor, the fundamental requirement is preserving the aqueous environment for cell. Without liquid thickness control, the medium solution dried out within 40 min—or even faster when humidity became lower—thus cell state altered a lot (Fig. S2). Such working time instability was one of the main disadvantages for gas phase odor biosensor without liquid thickness control. To compensate for the water evaporation in cell area, the pump A infused additional buffer solution for liquid thickness control. Hence, the cell state remained normal with a little reduction in fluorescence intensity owing to photobleaching after 75 min (Fig. S3).

For further assessing the effect of maintaining liquid layer, 0.4 s 1% 1-octen-3-ol vapor stimulations were supplied (Fig. 3). The percentage here means the dilution ratio of the analyte in the vial. Although the cell lifespan was considerably lengthened, the final response time of biosensor remained similar to that without liquid thickness control. This was coincident with other researchers' results that OR response diminished and terminated even if the liquid still existed in the biosensor (Sato and Takeuchi, 2014). Only liquid thickness control is insufficient for extending the lifetime of our biosensor. The compensated buffer solution had multiple chemical components while only water evaporated from cell area causing the ion density to increase with time. Meanwhile, there was no method to eliminate the residual odorant molecules from previous stimulations. Therefore, refreshing the buffer solution during experiment is highly demanded for further prolonging the lifespan of odor biosensor.

3.3. Extension of sensor lifetime by exchanging liquid

To overcome the ion and odor accumulation problem, the liquid exchange was introduced. Here, pump B withdrew liquid at 3 step/tick all the time, pump A injected buffer solution to maintain the impedance

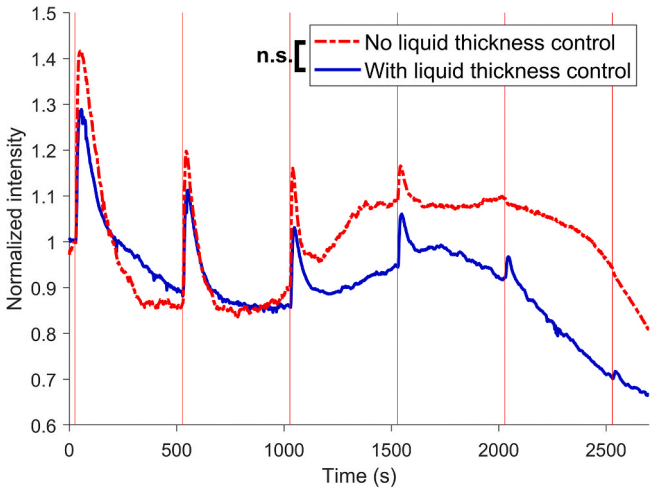

Fig. 3. OR reacts to 0.4 s 1% 1-octen-3-ol with or without liquid thickness control, red vertical line indicates the timing of vapor exposure, the fluorescence curve is normalized based on the intensity when first stimulation was applied. OR responses from 1st to 6th stimulations have no significant difference according to the two-sample *t*-test. (For interpretation of the references to colour in this figure legend, the reader is referred to the Web version of this article.)

value. The Pump A infusion speed was determined by microcontroller output signal, its normal value was 4–6 step/tick according to various room humidity. 0.4 s 1% 1-octen-3-ol headspace gas was chosen as stimulus. Fig. S4 shows OR responded to its agonist until 24th stimulation at 11539 s with 3 step/tick liquid exchange while the response from no liquid exchange ceased after 6th stimulation at 2532 s. The lifetime of biosensor was significantly extended, but the magnitude of response shrank with time obviously.

Considering that the entire liquid exchange volume between two adjacent stimulations was 3.97 μl which was insufficient for replacing all medium in cell area, we repeated experiments under various liquid displacement rates and obtained their responses. Fig. 4 reveals that even the minimum liquid exchange velocity was capable of prolonging the sensor lifespan. Even though all results had the dropping tendency of response magnitude with time, faster liquid flow speed always

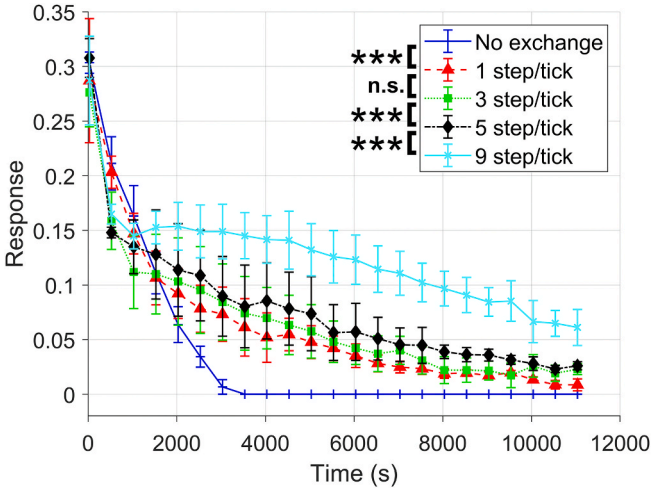

Fig. 4. OR response under different liquid exchange speed, each mark in the figure represents the OR response obtained in the relevant time, each flow speed (0, 1, 3, 5, 9 step/tick) experiment was repeated 3 times, the error bar represents the mean ± SEM of response. Based on two-sample *t*-test, most batches of adjacent OR response results have significant difference, ***$p < 0.001$, $N = 23$.

conducted stronger response in overall view. Most batches of response results have significant differences with each other. The OR response of 23rd stimulation under 9 step/tick liquid exchange speed suggests the lifetime of this odor biosensor would be much longer than 3 h. However, limited by the pump volume, the experiment terminated before OR response dropping to zero.

We can imagine that if the liquid replacement rate is accelerated more, the response curve also upper shifts synchronously. Meanwhile, faster liquid exchange velocity removes more odorant molecules before they combine with OR to trigger the calcium ion influx. Hence, such promotion surely reaches to its zenith under a specific rate. After that, the improvement acquired from less odor accumulation is weaker than the attenuation caused by smaller odorant concentration, causing the response curve to lower shift with flow rate.

3.4. Enhance the OR response by exchanging liquid intermittently

Since the continuous liquid exchange eliciting odorant molecules might decrease the OR response, we suspended the liquid flow 30 s before and started the flow again 70 s after stimulation, namely, only executing liquid exchange from 70 s to 470 s since last stimulation (Fig. 5a). In order to retain approximate liquid exchange volume, the flow rate was set to 12 step/tick. Fig. 5b demonstrates the intermittent liquid exchange enhanced the OR response towards 0.4 s 1% 1-octen-3-ol vapor stimulation distinctly from 1st to 13th stimulations. Since 14th stimulation, the response became similar. It means in the beginning, no liquid flow allowed odorant concentration reached to higher level resulting in larger response; after several cycles, the odor accumulation and fluorescent protein response decay dominated the OR response, even if no odorant molecules were flushed away from cell area during stimulation period, the enhancement in 1-octen-3-ol concentration could not introduce significant difference anymore. The choice between continuous and intermittent flow should be determined according to specific application scenarios. When researchers intend to detect tiny volume of low concentration odorant sample, intermittent flow method with its higher sensitivity is preferred. On the other hand, if scientists want to continuously monitor some materials, continuous flow method with its more stable response is admired.

Besides the remarkable improvement brought from intermittent liquid exchange, the side effect of this method is also described as follows. Fig. 5c depicts the impedance curve of continuous and intermittent flow. The continuous flow impedance curve remained quite stable in the process of whole test except a short period at the outset. The intermittent flow impedance curve, however, vibrated once the liquid flow was paused or resumed although the absolute value of those fluctuations were still minor, and the amplitude of such undulation elevated with time. We believe the intermittent flow influenced the solution volume in cell area and thus the impedance changed. Fortunately, unlike the impedance curve, no visible artifact was observed in fluorescence intensity curve owing to intermittent flow (Fig. S5). For extenuating the

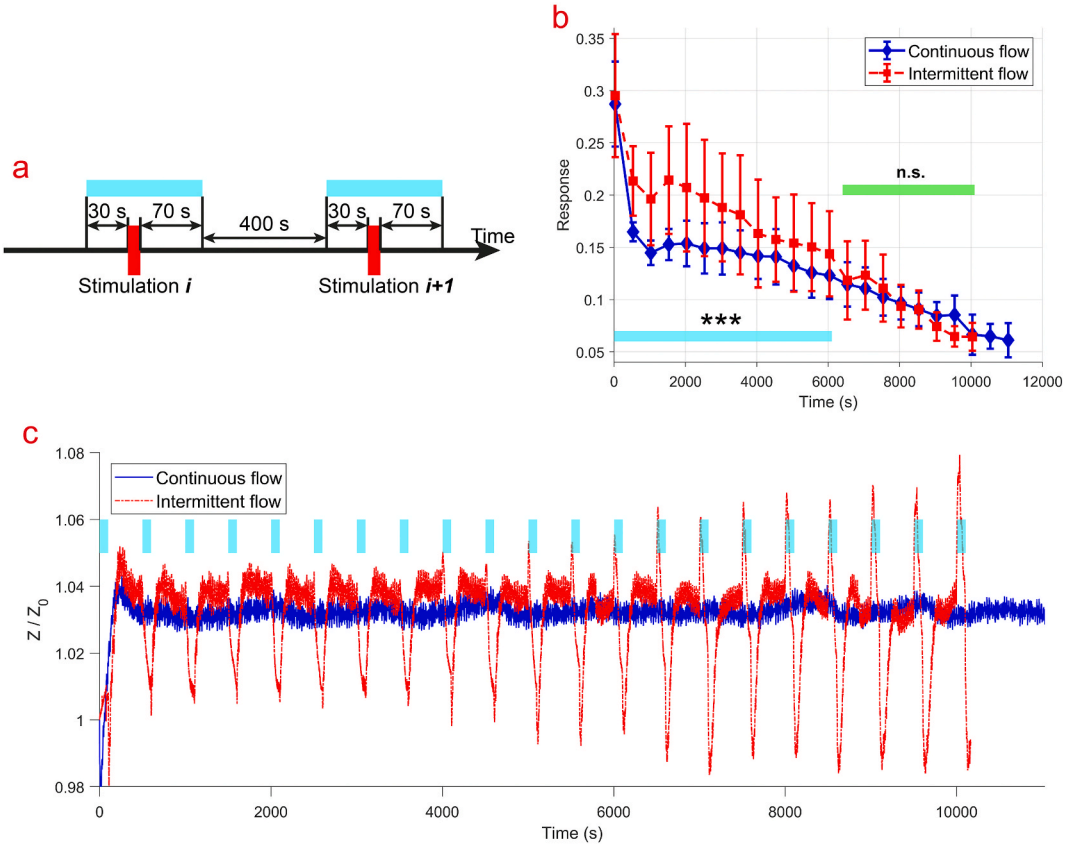

Fig. 5. Difference between continuous and intermittent liquid exchange. (a) Illustration of intermittent liquid exchange. Red vertical bar indicates the timing of odorant stimulation. Cyan horizontal bar indicates the timing of no liquid flow. (b) OR responses under continuous or intermittent liquid exchange, each mark in the figure represents the OR responses obtained in the corresponding time, the experiment for each condition was repeated 3 times, the error bar represents the mean ± SEM of response, the intermittent flow curve terminated after 21st stimulation because ran out of buffer solution in syringe pump. Based on the two-sample *t*-test, during the time range of cyan horizontal bar (1st to 13th stimulations), the OR responses have significant difference, ***$p < 0.001$; during the period of green horizontal bar (14th to 21st stimulations), the OR responses have no significant difference. (c) Impedance curve of continuous and intermittent flow. Cyan vertical bar indicates the timing of no liquid flow of intermittent liquid exchange, the intermittently flow curve terminated after 21st stimulation because ran out of buffer solution in syringe pump, Z is the impedance value in corresponding time, Z_0 is the initial impedance value. (For interpretation of the references to colour in this figure legend, the reader is referred to the Web version of this article.)

fluctuations in impedance curve, we may execute the same volume of liquid exchange within a cycle by extending the interval between two stimulations and reducing the flow velocity.

3.5. Odorant concentration dependency

To evaluate the sensor response towards various concentrations of target odorant, the 1-octen-3-ol liquid samples were prepared from 100% to 0.0001% (*v*/*v*) by 10-fold dilution and the 0.4 s headspace gas of each density was supplied to cell five times. The liquid exchange was set to 9 step/tick continuous flow. Fig. 6 shows a sigmoidal response curve with 1-octen-3-ol concentration from 1×10^{-3}%–100% while the magnitude of 1×10^{-4}% and 1×10^{-3}% odorant stimulation responses is similar. Herein, the maximum response emerged under pure 1-octen-3-ol headspace vapor stimulation. But we believe larger amount of target ligand such as extending the odorant stimulation duration longer than 0.4 s will introduce better response. The response obtained here was larger than our previous research (Deng et al., 2021). There are two main reasons: Firstly, the interval of two stimulations extended from 180 s to 500 s, so the fluorescent curve could recover to a relatively steady level which made the response of individual stimulation more independent from each other, allowing larger brightness increase margin for next stimulation. Secondly, the liquid exchange removed residual odorant molecules from previous stimulation, making the baseline lower for subsequent stimulations. Therefore, we assert that maintaining the liquid thickness and exchanging liquid benefit our odor biosensor at lifetime and sensitivity.

This odor biosensor response curve also demonstrates the reason why OR response diminishes with odorant accumulation. At the very beginning, no 1-octen-3-ol molecule existed in cell area, the agonist concentration increased from zero to a specific level when it was exposed to first stimulation thus resulting in a distinct response. After several stimulations, the residual odorant molecules made the relative increase which was attributed to odorant stimulation shrank significantly. Therefore, the OR response diminished or even became invisible.

4. Conclusion

In this study, a gas phase odor biosensor based on cell expressing Or13a combined with liquid thickness control and liquid exchange method was developed. A feedback control structure was employed for fine control of its thickness. A pair of electrodes with impedance measurement circuit was utilized for measuring the impedance value in real time due to their low cost, small size, and ease of integration. The optimal working frequency and liquid volume were determined according to the impedance alteration during liquid evaporation. It was confirmed that the liquid thickness control was able to extend the lifetime of cell considerably but only made a limited contribution to longer lifetime of biosensor. Then, the liquid exchange was introduced, and even the minimum liquid exchange velocity could prolong the lifetime of senor obviously. With the increasing liquid exchange rate, the overall response curve had an upward trend so better response was obtained. For further improving the sensor sensitivity, the intermittent liquid flow was applied. It enhanced the OR response towards the first several stimulations. After a series of stimulations, however, it could not eliminate the influence of fluorescent protein photobleaching and odor accumulation. Thus the enhancement in OR response disappeared. The Or13a responses towards various concentrations of 1-octen-3-ol vapor here were better than our previous research demonstrating the advantages brought from liquid thickness control and liquid exchange. With the liquid thickness control and liquid exchange, our odor biosensor can respond to odorant stimulations for enough long time. We believe those methods broaden the application scenarios and improve the capacity of odor biosensor in gas phase odorant detection.

Meanwhile, the liquid thickness control method here is suitable for applying in other research aspects which require maintaining the water or moist state of object (Ali et al., 2021; Buznikov et al., 2018; Buznikov and Kurlyandskaya, 2021; Liu et al., 2012; Mech-Dorosz et al., 2021; Wang et al., 2017). In addition, the early stop of OR response towards target odorant stimulation suggests that the olfactory fatigue might be caused by saturated concentration of residual odorant molecules from previous breath in human nasal mucus.

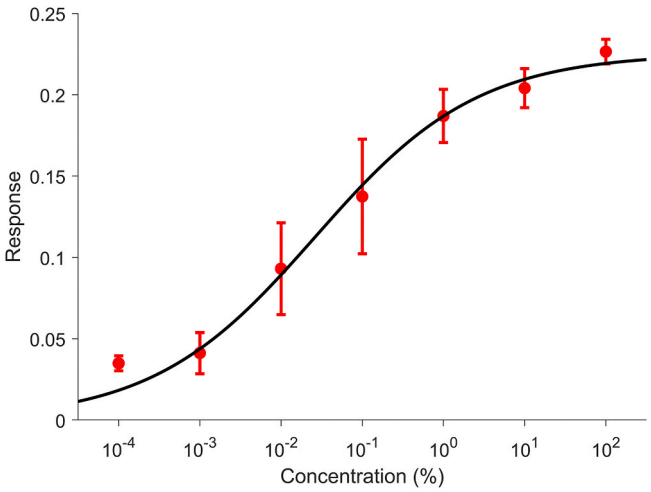

Fig. 6. Sample concentration dependency of Or13a towards 1-octen-3-ol. The horizontal axis concentration is the 1-octen-3-ol liquid sample concentration from 10^{-4}%–100% (v/v). The bar represents the mean ± SEM of response, n = 5.

To further enhance the performance of liquid thickness control and liquid exchange, we can design a microfluidic channel for more thorough liquid exchange. Also forming an electrode array on the surface of transparent material is capable of precisely detecting liquid thickness level at thinner than 100 μm which allows the biosensor system to work under extreme thin liquid level (Thiele et al., 2009). However, this study is the fundamental research about extending the lifetime of odor biosensors extendable to better performance.

CRediT authorship contribution statement

Hongchao Deng: Methodology, Software, Formal analysis, Investigation, Writing – original draft, Visualization, Funding acquisition. **Hidefumi Mitsuno:** Methodology, Investigation, Resources, Writing – review & editing. **Ryohei Kanzaki:** Methodology, Resources, Writing – review & editing. **Takamichi Nakamoto:** Conceptualization, Methodology, Writing – review & editing, Project administration, Funding acquisition.

Declaration of competing interest

The authors declare that they have no known competing financial interests or personal relationships that could have appeared to influence the work reported in this paper.

Acknowledgements

This work was supported in part by JSPS KAKENHI under Grant JP18H03773.

Appendix A. Supplementary data

Supplementary data to this article can be found online at https://doi.org/10.1016/j.bios.2021.113887.

References

Ali, A., Shah, T., Ullah, R., Zhou, P., Guo, M., Ovais, M., Tan, Z., Rui, Y.K., 2021. Front. Chem. 9, 548.

Buznikov, N.A., Kurlyandskaya, G.V., 2021. Sensors 21, 5151.

Buznikov, N.A., Safronov, A.P., Orue, I., Golubeva, E.V., Lepalovskij, V.N., Svalov, A.V., Chlenova, A.A., Kurlyandskaya, G.V., 2018. Biosens. Bioelectron. 117, 366–372.

Chen, T.W., Wardill, T.J., Sun, Y., Pulver, S.R., Renninger, S.L., Baohan, A., Schreiter, E. R., Kerr, R.A., Orger, M.B., Jayaraman, V., Looger, L.L., Svoboda, K., Kim, D.S., 2013. Nature 499, 295–300.

Da Silva, M.J., Schleicher, E., Hampel, U., 2007. Meas. Sci. Technol. 9, 533–540.

Datta-Chaudhuri, T., Araneda, R.C., Abshire, P., Smela, E., 2016. Sensor. Actuator. B Chem. 235, 74–78.

Deng, H., Mitsuno, H., Kanzaki, R., Nakamoto, T., 2021. IEEE Sensor. J. 21, 21184–21191.

Ema, K., Yokoyama, M., Nakamoto, T., Moriizumi, T., 1989. Sensor. Actuator. 18, 291–296.

Hurlburt, E.T., Newell, T.A., Conditioning, A., 1995. Exp. Fluid 21, 357–362.

Johnson, D.C., 2011. N. Engl. J. Med. 364, 978.

Kanja, J., Mills, R., Li, X., Brunskill, H., Hunter, A.K., Dwyer-Joyce, R.S., 2021. Ultrasonics 110, 106291.

Khadka, R., Aydemir, N., Carraher, C., Hamiaux, C., Colbert, D., Cheema, J., Malmström, J., Kralicek, A., Travas-Sejdic, J., 2019. Biosens. Bioelectron. 126, 207–213.

Kida, H., Fukutani, Y., Mainland, J.D., de March, C.A., Vihani, A., Li, Y.R., Chi, Q., Toyama, A., Liu, L., Kameda, M., Yohda, M., Matsunami, H., 2018. Nat. Commun. 9, 4556.

Leal, W.S., 2013. Annu. Rev. Entomol. 58, 373–391.

Lee, S.H., Oh, E.H., Park, T.H., 2015. Biosens. Bioelectron. 74, 554–561.

Lim, J.H., Park, J., Ahn, J.H., Jin, H.J., Hong, S., Park, T.H., 2013. Biosens. Bioelectron. 39, 244–249.

Liu, R., Jin, C., Song, F., Liu, J., 2012. Int. J. Nanomed. 8, 33–38.

Mech-Dorosz, A., Khan, M.S., Mateiu, R.V., Hélix-Nielsen, C., Emnéus, J., Heiskanen, A., 2021. Electrochim. Acta 373, 137917.

Mitsuno, H., Sakurai, T., Namiki, S., Mitsuhashi, H., Kanzaki, R., 2015. Biosens. Bioelectron. 65, 287–294.

Mujiono, T., Sukekawa, Y., Nakamoto, T., Mitsuno, H., Termtanasombat, M., Kanzaki, R., Misawa, N., 2017. Sensor. Mater. 29, 65–76.

Münch, D., Galizia, C.G., 2016. Sci. Rep. 6, 21841.

Nakamoto, T., 2016. Olfactory display and odor recorder. In: Nakamoto, T. (Ed.), Essentials of Machine Olfaction and Taste. John Wiley & Sons Singapore Pte Ltd, Singapore, pp. 247–314.

Nielsen, B.L., Rampin, O., Meunier, N., Bombail, V., 2015. Front. Neurosci. 9, 226.

Pearce, T.C., Schiffman, S.S., Nagle, H.T., Gardner, J.W., 2002. Handbook of Machine Olfaction: Electronic Nose Technology. Wiley-VCH.

Persaud, K., Dodd, G., 1982. Nature 299, 352–355.

Sato, K., Takeuchi, S., 2014. Angew. Chem. Int. Ed. 53, 11798–11802.

Su, X., Chen, D., Li, N., Stevenson, A.C., Li, G., Hu, R., 2020. Sensors Actuator A Phys. 305, 111938.

Sukekawa, Y., Mitsuno, H., Kanzaki, R., Nakamoto, T., 2021. Biosens. Bioelectron. 179, 113053.

Sukekawa, Y., Mitsuno, H., Kanzaki, R., Nakamoto, T., 2019. IEEE Sensor. J. 19, 7192–7200.

Termtanasombat, M., Mitsuno, H., Misawa, N., Yamahira, S., Sakurai, T., Yamaguchi, S., Nagamune, T., Kanzaki, R., 2016. J. Chem. Ecol. 42, 716–724.

Thiele, S., Silva, M.J. Da, Hampel, U., 2009. IEEE Sensor. J. 9, 533–540.

Wang, T., Zhou, Y., Lei, C., Luo, J., Xie, S., Pu, H., 2017. Biosens. Bioelectron. 90, 418–435.

Wu, C., Chen, P., Yu, H., Liu, Q., Zong, X., Cai, H., Wang, P., 2009. Biosens. Bioelectron. 24, 1498–1502.